Supporting Material for:

Integrin Generated Forces Lead to Streptavidin-Biotin Unbinding in Cellular Adhesions

Carol Jurchenko, Yuan Chang, Yoshie Narui, Yun Zhang, Khalid S. Salaita
Department of Chemistry, Emory University, Atlanta, GA, USA

This file includes:


Supporting Methods

Supporting Figures 1-14

Supporting Methods:

1. Quantitative fluorescence calibration procedure. DOPE-Alexa 647 lipids were used to create a calibration curve (Fig. S4) in which the number of DOPE-Alexa 647 molecules was correlated to the fluorescence intensity of a supported lipid bilayer (SLB) surface (*1*). The SLB was composed of 1,2-dioleoyl-*sn*-glycero-3-phosphocholine (DOPC) (Avanti Polar Lipids) doped with DOPE-Alexa 647 at concentrations that ranged from 0.016 mol percent to 0.24 mol percent.

DOPE (1,2-di-(9Z-octadecenoyl)-*sn*-glycero-3-phosphoethanolamine) lipids were purchased from Avanti Polar Lipids. For the DOPE-Alexa 647 synthesis, the limiting reagent was the reactive Alexa Fluor 647 NHS ester; therefore the reaction was carried out at a 1:1 ratio of fluorophore to lipid molecule. From a 10 mg/ml DOPE solution in chloroform, 38.9 µl (MW=743.5 g/mol, 523 nmol) was transferred to a 2 ml glass vial. The organic solvent was evaporated off under a stream of ultrapure N_2 for ~15 min. The dry lipid film was redissolved in 38.9 µl of dry DMF. A 0.1 M solution of triethylamine in DMF was prepared and 1.5 fold molar excess (7.86 µl) was added to the lipid solution. The reactive dye (0.5 mg, 523 nmol) was resuspended in 5 µl of DMF and slowly added to the lipid mixture. A small teflon stirbar was added to the reaction, which was capped, protected from light and allowed to stir overnight at room temperature.

After 16 h, the solution was transferred to a 1.5 ml microcentrifuge tube and spun down to dryness on a Speedvac. The reaction mixture was resuspended in chloroform and transferred to a 20 ml glass vial; both the free dye and the lipid-dye conjugate are soluble in chloroform. The solution was then dried on a rotovap and resuspended in 2 ml of hexane (HPLC grade). The mixture was sonicated briefly (2-3 seconds) until all components were in solution and allowed to sit on the bench undisturbed for 10-15 min as the unreacted dye precipitated out of solution. The soluble fraction containing the lipid-dye conjugate was collected and transferred into a clean 20 ml glass vial, and this process was repeated 3 times. During the fourth repeat, the hexane mixture was placed on ice for 1.5 h to promote precipitation of any remaining free dye. The solution was then dried down on a rotary evaporator and resuspended in 500 µl of chloroform for further use.

After each transfer, TLC was used to check for the presence of free dye. A solvent mixture of chloroform/methanol/water/concentrated ammonium hydroxide (6/3.4/0.55/0.05) was used for analysis. The final solution showed no visible trace of free dye as seen in the image of the TLC plate (below). The final mass of the product (1584 amu) was observed in MALDI-TOF using negative ion mode with 0.5 M dihydroxybenzoic acid in methanol as the matrix. The yield ranged from 5-10 nmol of DOPE-Alexa 647 (according to ε_{650} = 239,000 cm^{-1} M^{-1}) resulting in a 1-2% overall yield. After synthesis and purification of the final product, the lipids were extruded through a 0.1 µm filter using a Mini-Extruder (Avanti Polar Lipids).
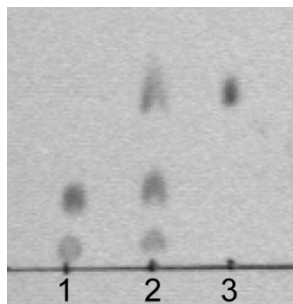
Photograph of TLC plate collected after the final stage of purification indicating no free dye present in the final lipid-dye product. Lane 1 = free dye, lane 2 = co-spot (free dye and lipid-dye conjugate), lane 3 = lipid-dye conjugate.

Once a series of SLB surfaces were made using DOPE-Alexa 647 at concentrations varying from 0.016 mol percent to 0.24 mol percent, the calibration curve was created and an F-factor (Eqn. 1) was determined where $I_{soln(protein\ conj.)}$ is the fluorescence intensity in bulk solution of the streptavidin- Alexa 647 conjugate and $I_{soln(lipid\ conj.)}$ is the intensity of an equal concentration of DOPE-Alexa 647 in solution.

$$F = \frac{I_{soln(protein\ conj.)}}{I_{soln(lipid\ conjugate)}}$$

Equation 1

The F-factor corrects for any change that may occur in the fluorophore intensity as a result of the conjugation and therefore allows the density of streptavidin-Alexa 647 on the surface to be determined using the DOPE-Alexa 647 calibration. A second F-factor was also measured for a cRGDfK(C)-Alexa 647-PEG$_{24}$-biotin conjugate in order to compare the fluorescence intensity of surfaces with Alexa 647 labeled cRGD to Alexa 647 labeled streptavidin surfaces and thereby determine a binding ratio of the sensor conjugate to surface streptavidin.

The fluorescence intensity of the sample was then calibrated using Eqn. 2,

$$I_{cal} = \frac{I_{sample}}{F}$$

Equation 2

where I_{sample} is the fluorescence intensity of the biotin functionalized surfaces containing streptavidin-Alexa 647 and F is the F-factor.

The calibrated sample intensity (I_{cal}) was then converted to number of fluorescent molecules on the sample surface by dividing it by the slope of the DOPE- Alexa 647 calibration curve (Fig. S4).

2. Förster distance between Alexa 647 and QSY21.
To verify the R_0 value between Alexa 647 and QSY21 we designed two calibration experiments (A and B). In the first set of experiments (Calibration A), the quencher was conjugated to streptavidin that was anchored to a supported lipid bilayer. The fluorophore was conjugated to the 5' terminus of a DNA duplex that was then bound to the streptavidin surface through a biotin group at the second 5' terminus. The distance between Alexa 647 and QSY21 was adjusted by changing the length (number of base pairs) of the DNA duplex (Fig. S9). Note that the base pair composition of the 5' ends of the duplex were maintained (GCC or CAC) throughout each duplex such that the local dye environment remained relatively constant (*2*).

The fluorophore-quencher distance was determined using the following equation,

$$\text{Distance } (r) = 0.34(N - 1) + L \qquad\qquad \text{Equation 3}$$

where N represents the number of base pairs in the DNA duplex, and L is the distance added by the fluorophore and biotin attachment linkers at the 5' ends of the DNA strands (*3, 4*) as well as the streptavidin radius (as estimated by the crystal structure PDB: 1SWB). The final value of L was estimated to be 3.3 nm with 1.3 nm estimated for the combined linker lengths and 2 nm for the streptavidin radius.

In calibration B, the Förster radius (R_0) of Alexa 647 and QSY21 was determined using DNA hairpin structures of varying lengths (Fig. S10). Each hairpin strand was converted from the closed state (high quenching efficiency) to the open state (decreased quenching efficiency) by adding the complementary strand. The distance between fluorophore and quencher was calculated using Eqn. 3, where L in this case represents the theoretical distance parallel to the DNA helical axis separating Alexa 647 and QSY21 for the case that n=1. The final value of L was estimated to be 1.3 nm for the combined fluorophore linker lengths (*3, 4*).

The R_0 values obtained from the two calibrations were then averaged to get a final R_0 value of 6.8 nm. This value is close to the 6.9 nm Förster distance reported by the manufacturer.

Calibration A to obtain the Förster distance of Alexa 647 and QSY21. The following DNA oligonucleotides were purchased from Integrated DNA Technologies (Coralville, IA):

12 mer
5'- /5Biosg/ GCC AGA GCA GTG -3'
5'- /5AmMC6/ CAC TGC TCT GGC -3'

16 mer
5'- /5Biosg/ GCC TAG AGC ATC AGT G -3'
5'- /5AmMC6/ CAC TGA TGC TCT AGG C -3'

21 mer
5'- /5Biosg/ GCC TAT GAA TGA GCT TCA GTG -3'
5'- /5AmMC6/ CAC TGA AGC TCA TTC ATA GGC -3'

33 mer
5'- /5Biosg/ GCC TAT ATA GTC ATC AGC CGT ATA GCA TCA GTG -3'
5'- /5AmMC6/ CAC TGA TGC TAT ACG GCT GAT GAC TAT ATA GGC -3'

Each of the amine functionalized oligonucleotides were labeled with Alexa 647 by adding 2.5 μl of 10x PBS and 2.5 μl of 1 M sodium bicarbonate to 20 μl of 1 mM DNA. An 8-fold molar excess of Alexa 647 NHS ester was then resuspended in 5 μl of dimethylformamide and added to the DNA mixture. The reaction was placed on a shaker (300 r.p.m.) and allowed to shake overnight at room temperature. The final product was purified by reverse phase HPLC with monitoring at 260 and 647 nm. The reaction mixture was injected through a 5 μm, 4.6 × 250 mm C_{18} column at a flow rate of 1 ml/min with a linear gradient of 10 – 60% B over 50 min (A: aqueous 0.1 M triethylammonium acetate buffer; B: acetonitrile (LC-MS Chromasolv, ≥99.9%; Fluka). This elution gradient was followed by a second gradient of 60 – 100 % B over 10 min to collect the more hydrophobic fractions.

Recombinant streptavidin was labeled with QSY21 by mixing 100 μg of the protein (2 mg/ml) in PBS (10 mM phosphate buffer, 137 mM NaCl, pH 7.4) with 5 μl of 1 M sodium bicarbonate and a 5-fold molar excess of QSY 21 NHS ester (Life Technologies). The reaction was allowed to proceed for 30 min at room temperature on a rotating platform. Purification was performed using a Slide-a-Lyzer Mini dialysis column (Thermo Fisher) with a MW cutoff of 3,500 g/mol. The average labeling ratio of the final product was determined to be 1.7 by UV-visible absorbance measurement.

In order to generate supported lipid bilayers, we prepared a lipid mixture consisting of 99.9% 1,2-dioleoyl-*sn*-glycero-3-phosphocholine (DOPC, Avanti Polar Lipids) and 0.1% 1,2-dioleoyl-*sn*-glycero-3-phosphoethanolamine-N-(cap biotinyl) (sodium salt) (DPPE-biotin, Avanti Polar Lipids). After mixing the lipids in the correct proportions in chloroform, the solution was dried with a rotary evaporator and placed under a stream of N_2 to ensure complete evaporation of the solvent. These lipid samples were then resuspended in Nanopure water and subjected to 3 freeze/thaw cycles by alternating immersions in an acetone and dry ice bath and a warm water bath (40 °C). To obtain small unilamellar vesicles (SUV's), lipids were extruded through a high pressure extruder with a 100 nm nanopore membrane (Whatman).

Supported lipid bilayers were assembled by adding SUV's to base etched 96 well plates with glass-bottomed wells. After blocking with BSA (0.1 mg/mL) for 60 min, bilayer surfaces were incubated with either unlabeled streptavidin (1 μg/400 μL) or streptavidin-QSY21 (1 μg/400 μL) for 1 h. Wells were rinsed 3 times with 5 mL of 1x PBS, then incubated with the appropriate DNA-Alexa 647 labeled duplex (200 nM) for 1 h and rinsed 3x with 5 mL of 1x PBS before imaging.

Calibration B to obtain the Förster distance of Alexa 647 and QSY21. Six different DNA hairpin sequences and complementary strands were designed and custom synthesized by Integrated DNA Technologies. The DNA sequence information is listed below:

Oligos	Hairpin Sequence	Complementary Sequence
QSY21 strand (contains biotin for anchoring via biotin-streptavdin and an amine for QSY21-NHS coupling)	5'-/5AmMC6/-CGC ATC TGT GCG GTA TTT CAC TTT – /3BioTEG/-3'	
Alexa 647 strand (contains amine for Alexa 647-NHS coupling)	5'- TTT GCT GGG CTA CGT GGC GCT CTT–/3AmMO/-3	
18mer	5'-GTG AAA TAC CGC ACA GAT GCG <u>TTT- CAT CTT TTG ATG -TTT</u> AAG AGC GCC ACG TAG CCC AGC -3'	5'- AAA CAT CAA AAG ATG AAA -3'
21mer	5'-GTG AAA TAC CGC ACA GAT GCG <u>TTT- CAT ACT TTT TGT ATG -TTT</u> AAG AGC GCC ACG TAG CCC AGC -3'	5'-AAA CAT ACA AAA AGT ATG AAA-3'
24mer	5'-GTG AAA TAC CGC ACA GAT GCG <u>TTT-GCT AGT TTT TTT TCT AGC -TTT</u> AAG AGC GCC ACG TAG CCC AGC -3'	5'-AAA GCT AGA AAA AAA ACT AGC AAA-3'
27mer	5'-GTG AAA TAC CGC ACA GAT GCG <u>TTT-CAG ACT TTT TTT TTT TGT CTG-TTT</u> AAG AGC GCC ACG TAG CCC AGC -3'	5'-AAA CAG ACA AAA AAA AAA AGT CTG AAA- 3'
37mer	5'-GTG AAA TAC CGC ACA GAT GCG <u>TTT-CGA TAC TTT TTT TTT TTT TTT TGT ATC G-TTT</u> AAG AGC GCC ACG TAG CCC AGC -3'	5'-AAA CGA TAC AAA AAA AAA AAA AAA AAA AGT ATC GAA A-3'
45mer	5'-GTG AAA TAC CGC ACA GAT GCG <u>TTT- CGA TAA CTT TTT TTT TTT TTT TTT TTT TTG TTA TCG -TTT</u> AAG AGC GCC ACG TAG CCC AGC -3'	5'- AAA CGA TAA CAA AAA AAA AAA AAA AAA AAA AAG TTA TCG AAA-3'

*Three thymine bases were added as a linker at the end of hairpin stem to increase the flexibility. The complementary strand hybridizes to both the 3-T linkers as well as the hairpin sequence.

The anchor arm was labeled with QSY21 and the upper arm was labeled with Alexa 647 (Fig. S10) by adding 1 μl of 1 mM DNA and 1 μl of 1 M sodium bicarbonate to 7 μl of PBS. Then, 1 μl of 10 mM Alexa 647-NHS ester (10-fold molar excess) was added to the DNA mixture. The reaction was allowed to incubate at room temperature overnight.

All the hairpins were anchored on the lipid membrane surface through a biotin-streptavidin interaction in 96-well plates with glass-bottomed wells. Supported lipid bilayers were assembled by adding small unilamellar vesicles (see above for synthesis) to base-etched 96-well plates. After blocking with BSA (0.1 mg/ml) for 30 min, bilayer surfaces were incubated with streptavidin (0.4 μg per well) for 1 h. Wells were then rinsed 3 times with 5

ml of PBS and incubated with the hairpin structure for 1 h. Finally, wells were rinsed 3 times with 5 ml PBS and imaged.

Quenching of the closed hairpin: In order to verify that the quenching of the fluorophore occurred when the hairpin was in the closed conformation, a solution fluorescence experiment was performed using the 37mer hairpin structure. The hairpin was formed and folded in 50 μl PBS at a concentration of 50 nM and the complementary strand was in 10-fold molar excess (500nM) to open the hairpin.
Denaturation step: 75 °C, 5 min
Renaturation step: temperature was allowed to return to room temperature at a rate of 4 ºC every 3 min.
When the hairpin hybridized with the complementary strand, we observed an increase in fluorescence signal (data not shown).

Förster distance of Alexa 647 and QSY21 calibration curve. The six hairpins were formed and folded in 50 μl PBS at 100 nM and the complementary strand was added in 10-fold molar excess (1000 nM) to open the hairpin.
Denaturation step: 75 °C, 5 min
Renaturation step: temperature was allowed to return to room temperature at a rate of 4 ºC every 3 min.
In this experiment, the longest hairpin (45mer, 15.38 nm) was used to determine the donor only intensity (the 0% energy transfer efficiency) in the calibration experiment.

3. Survival probabilities of molecular bonds in series
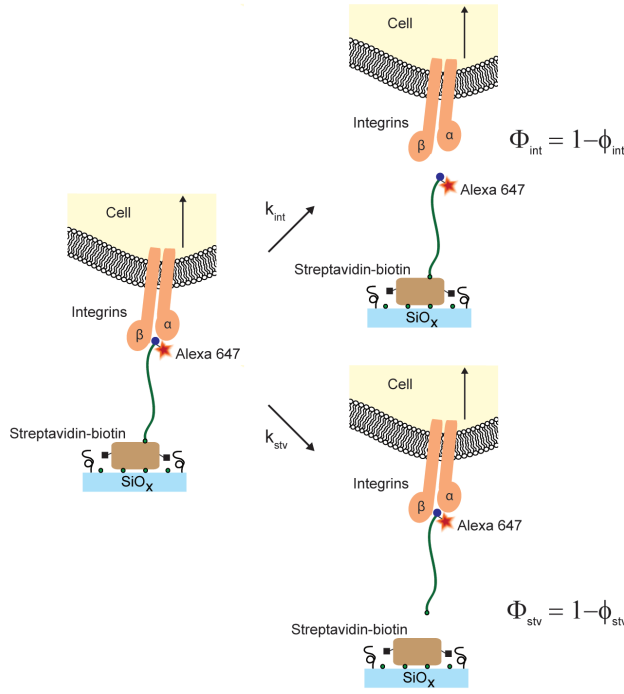
Schematic depiction of the possible dissociation outcomes when two bonds are in series.

When two bonds are found in a series and subjected to an external mechanical load, it is expected that the weaker bond will be more likely to dissociate. The probability of a single bond rupture event primarily depends on two parameters, the k_{off} rate at zero force and the distance required to displace the bond from its equilibrium bound state to the transition state, Δx. Likewise, when two bonds are placed in a series, the probability of weaker bond rupture will depend on the relative values of k_{off} (force = 0) and Δx. In order to more quantitatively calculate the probability of single bond dissociation when two bonds, such as streptavidin-biotin and integrin-ligand, are found in a series and placed under tension, we followed an in depth analysis originally developed by Neuert et $al.$ (5). First, we define the survival probability of each bond over time as follows,

$$\Phi_{stv}(t) = 1 - \varphi_{stv}(t) \qquad\qquad \text{Equation 4}$$

$$\Phi_{int}(t) = 1 - \varphi_{int}(t) \qquad\qquad \text{Equation 5}$$

where Φ_{stv} and Φ_{int} are the probabilities of streptavidin-biotin and integrin-ligand bond survival, respectively, and φ_{stv} and φ_{int} are the probabilities of the respective bonds rupturing (see figure above). In order to describe bond survivability under force, the Bell model (6), is used to reflect the k_{off} rates of the bonds under force,

$$k_{int}(f) = k_{int}(f = 0) \times e^{f \cdot \Delta x_{int}/k_B T} \qquad\qquad \text{Equation 6}$$

$$k_{stv}(f) = k_{stv}(f = 0) \times e^{f \cdot \Delta x_{stv}/k_B T} \qquad\qquad \text{Equation 7}$$

where f refers to the applied force, Δx_{stv} and Δx_{int} are the distances between the bound state and the transition state for streptavidin-biotin and integrin-ligand association, respectively. k_{stv} and k_{int} are the k_{off} rates for streptavidin-biotin and integrin ligand bonds, respectively. k_B is the Boltzmann constant and T is the absolute temperature.

Equations 4 and 5 can then, as described in Neuert *et al.*, be combined with Equations 6 and 7 to yield a mathematical model to describe the likelihood of bond dissociation under force.

In our case, the two bonds are highly asymmetric where k_{int} = 0.072 s^{-1}(*7*) and k_{stv} = ~3 x 10^{-5} at 37 °C (*8, 9*) (Fig. S7). Since the two bonds are linked, both bonds equally experience the applied tension, *f*. Furthermore, if we assume that Δx_{int} = Δx_{stv}, then the likelihood of bond dissociation is force and loading rate independent. In this case, the ratio k_{stv}/k_{int} remains constant for all values of *f* based on equations 6 and 7. Therefore, we can compare the k_{off} values under zero force and determine the probability of bond dissociation under integrin-mediated tension. Using the ratio of the reported off rates, the probability of streptavidin-biotin dissociation while maintaining integrin-ligand association is ~0.00003. This suggests that streptavidin-biotin would need to experience hundreds of thousands of cycles of mechanical force to dissociate through integrin-ligand mediated tension, which is unlikely based on the expected k_{on} values (*7, 10*) and the reported force oscillation frequency of 0.1 Hz (*11*).

In the situation where Δx of streptavidin-biotin is larger than that of the integrin-ligand bond (which is likely the case), the analysis becomes more complex, as the change in k_{off} becomes loading rate and force dependent. In general, large loading rates and greater magnitudes of tension favor the bond with smaller values of Δx. Nonetheless, in our case, the k_{off} values differ by orders of magnitude and will likely dominate Φ_{stv}.

A
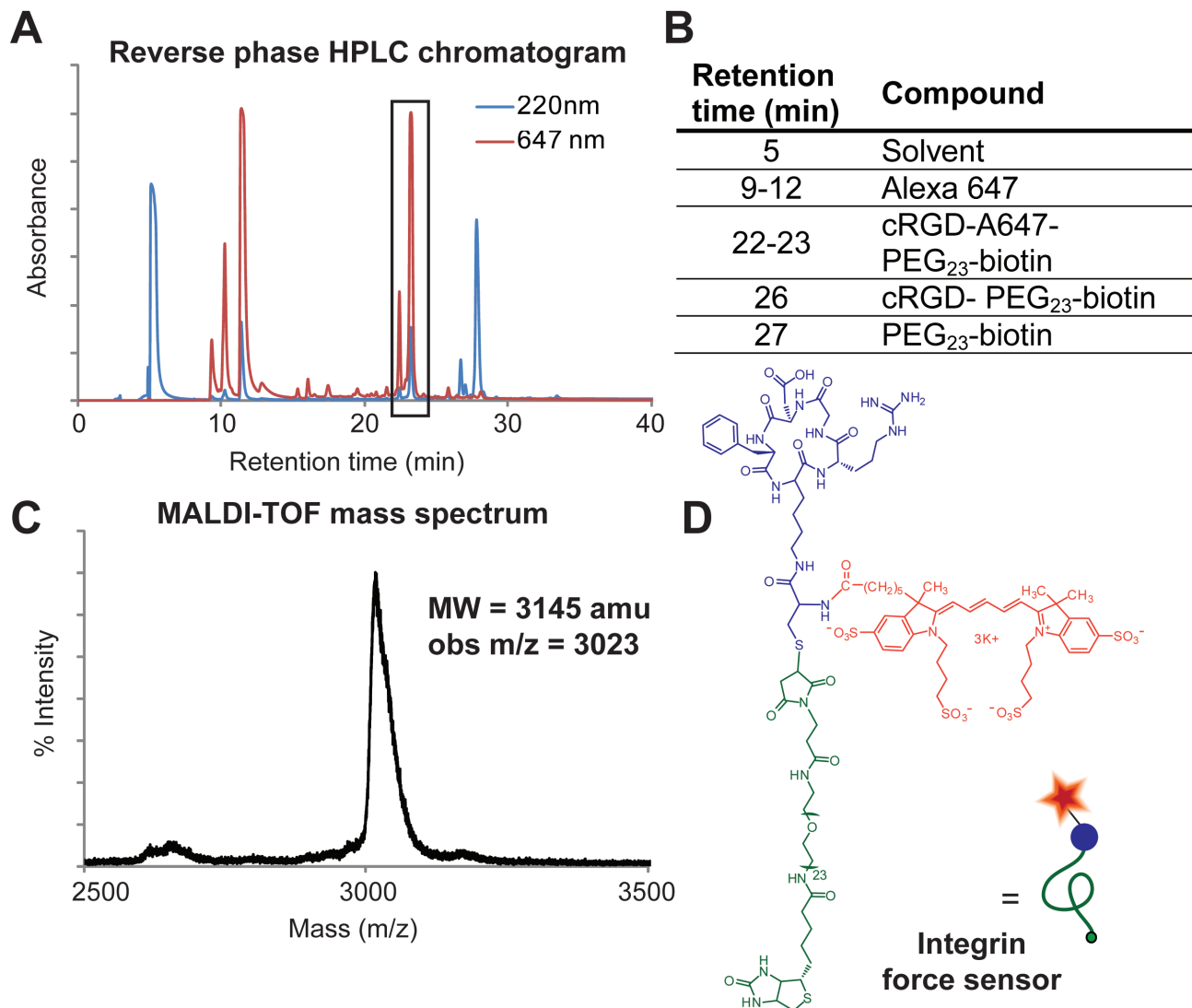
Reverse phase HPLC chromatogram

— 220nm
— 647 nm

Absorbance

Retention time (min)

B

Retention time (min)	Compound
5	Solvent
9-12	Alexa 647
22-23	cRGD-A647-PEG$_{23}$-biotin
26	cRGD- PEG$_{23}$-biotin
27	PEG$_{23}$-biotin

C

MALDI-TOF mass spectrum

MW = 3145 amu
obs m/z = 3023

% Intensity

Mass (m/z)

D

=

Integrin force sensor

Figure S1. Purification and characterization of the cRGDfK(C)-A647-PEG$_{23}$-biotin conjugate. (A-B) Reverse phase HPLC chromatogram of the Alexa 647 NHS, cRGDfK(C), biotin-PEG$_{23}$-maleimide reaction mixture. The absorbance was measured at 220 and 647 nm. 1 ml fractions were collected as they eluted off the column (flow rate = 1 ml/min). The peaks were characterized by MALDI-TOF MS (C) and the final integrin force sensor product (MW$_{obs}$ = 3023; MW$_{expected}$=3145) was found to elute at 22-23 min. (D) Structure of the final product.

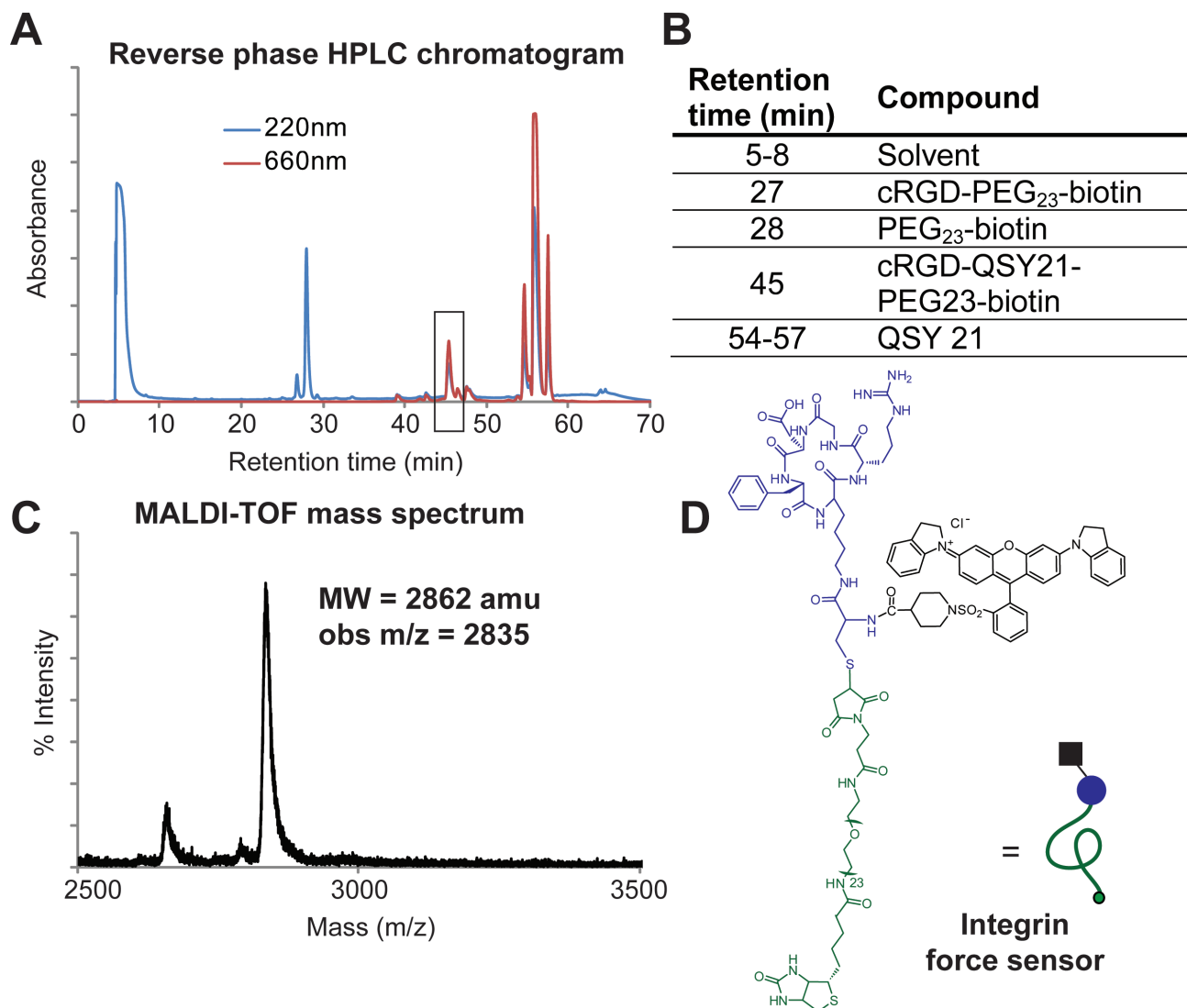**A** Reverse phase HPLC chromatogram

— 220nm
— 660nm

Absorbance vs Retention time (min)

B

Retention time (min)	Compound
5-8	Solvent
27	cRGD-PEG$_{23}$-biotin
28	PEG$_{23}$-biotin
45	cRGD-QSY21-PEG23-biotin
54-57	QSY 21

C MALDI-TOF mass spectrum

MW = 2862 amu
obs m/z = 2835

% Intensity vs Mass (m/z)

D

= Integrin force sensor

Figure S2. Purification and characterization of the cRGDfK(C)-QSY21-PEG$_{23}$-biotin conjugate. (A-B) Reverse phase HPLC chromatogram of the QSY21 NHS, cRGDfK(C), biotin-PEG$_{23}$-maleimide reaction mixture. The absorbance was measured at 220 and 660 nm. 1 ml fractions were collected as they eluted off the column (flow rate = 1 ml/min). The peaks were characterized by MALDI-TOF MS (C) and the final integrin force sensor product (MW$_{obs}$ = 2835; MW$_{expected}$=2862) was found to elute at 45 min. (D) Structure of the final product.
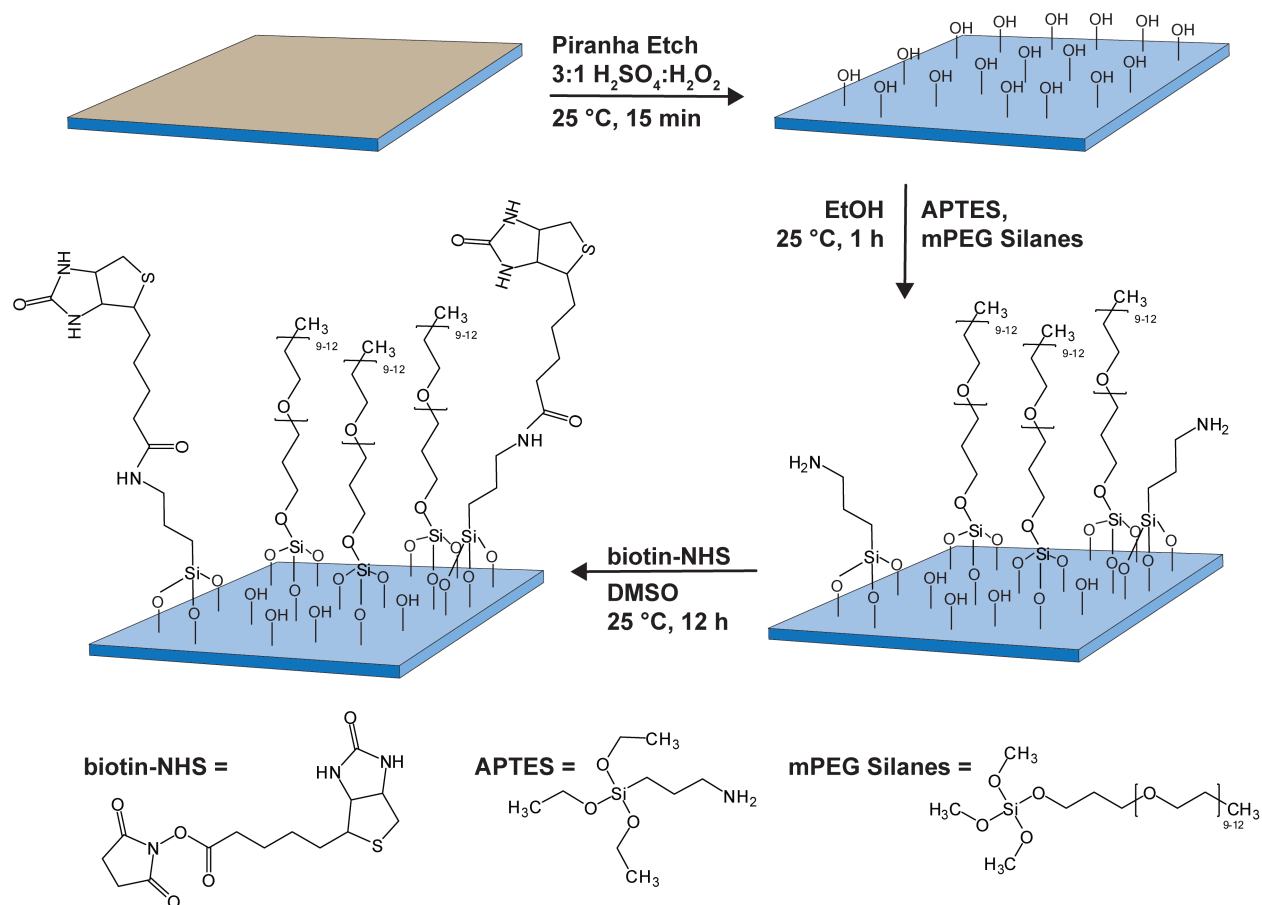
Figure S3. Scheme depicting the covalent biotin-functionalization of glass surfaces. Glass coverslips (as described in Materials and Methods) were piranha-etched in order to produce a clean glass surface containing free terminal hydroxyl groups. A binary mixture of APTES and mPEG silane at different ratios was coupled to the hydroxyl surface groups of the glass coverslip to generate varying ratios of reactive amine and passivating mPEG groups. In the final reaction step, biotin containing a reactive N-hydroxysuccinimide ester was coupled to the free amines on the surface.
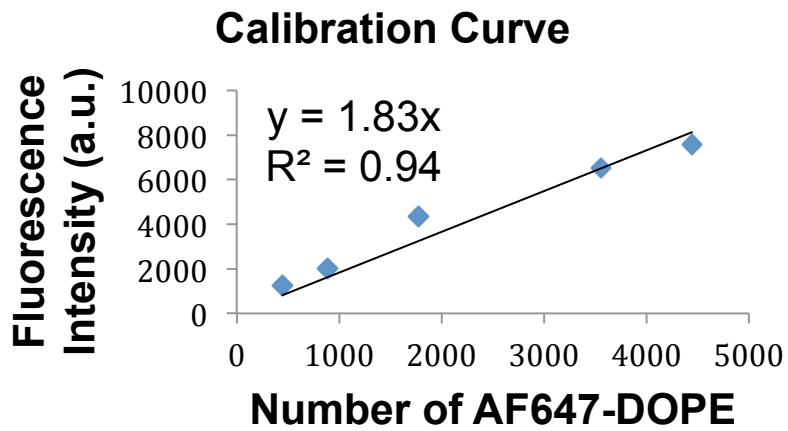
Calibration Curve

$y = 1.83x$
$R^2 = 0.94$

Figure S4. Quantitative fluorescence calibration to measure surface density of streptavidin and peptide mechanophore. Calibration showing the fluorescence intensity of DOPE-Alexa 647 doped DOPC supported lipid membrane (see Methods and Materials and Supporting Methods).
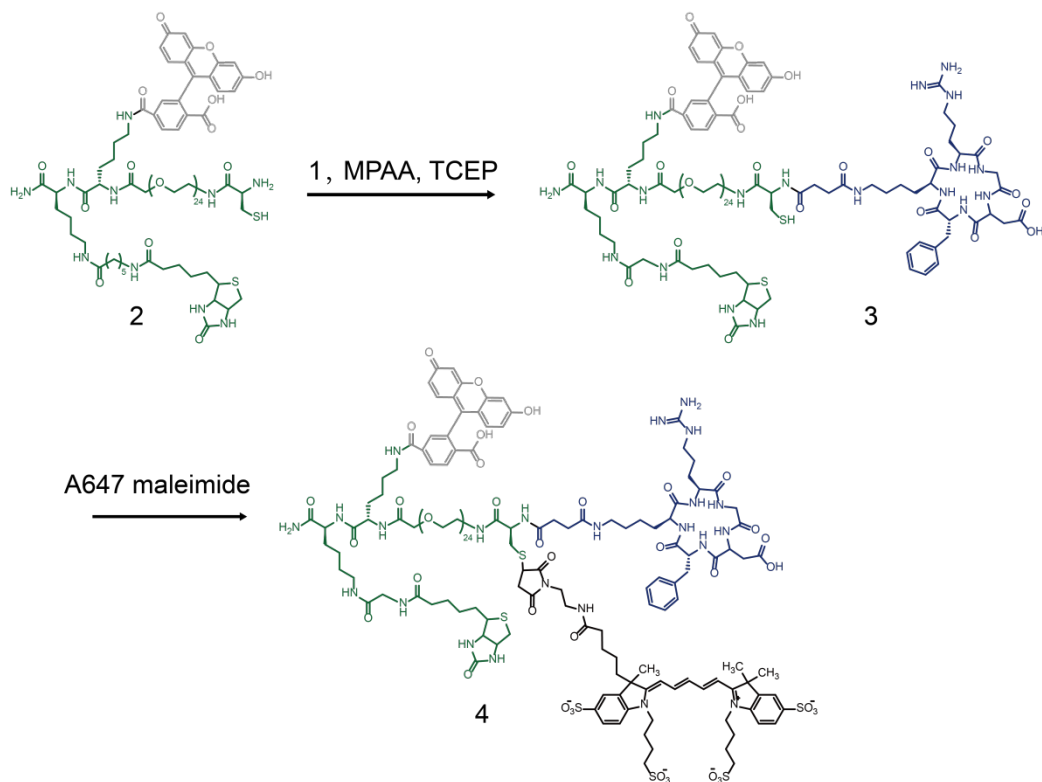
Figure S5. Conjugation of cRGDfK α-thioester with fluorescein-PEG₂₄-biotin conjugate and coupling of Alexa 647 as the acceptor fluorophore. Full synthesis is described in the Materials and Methods section in the main manuscript.
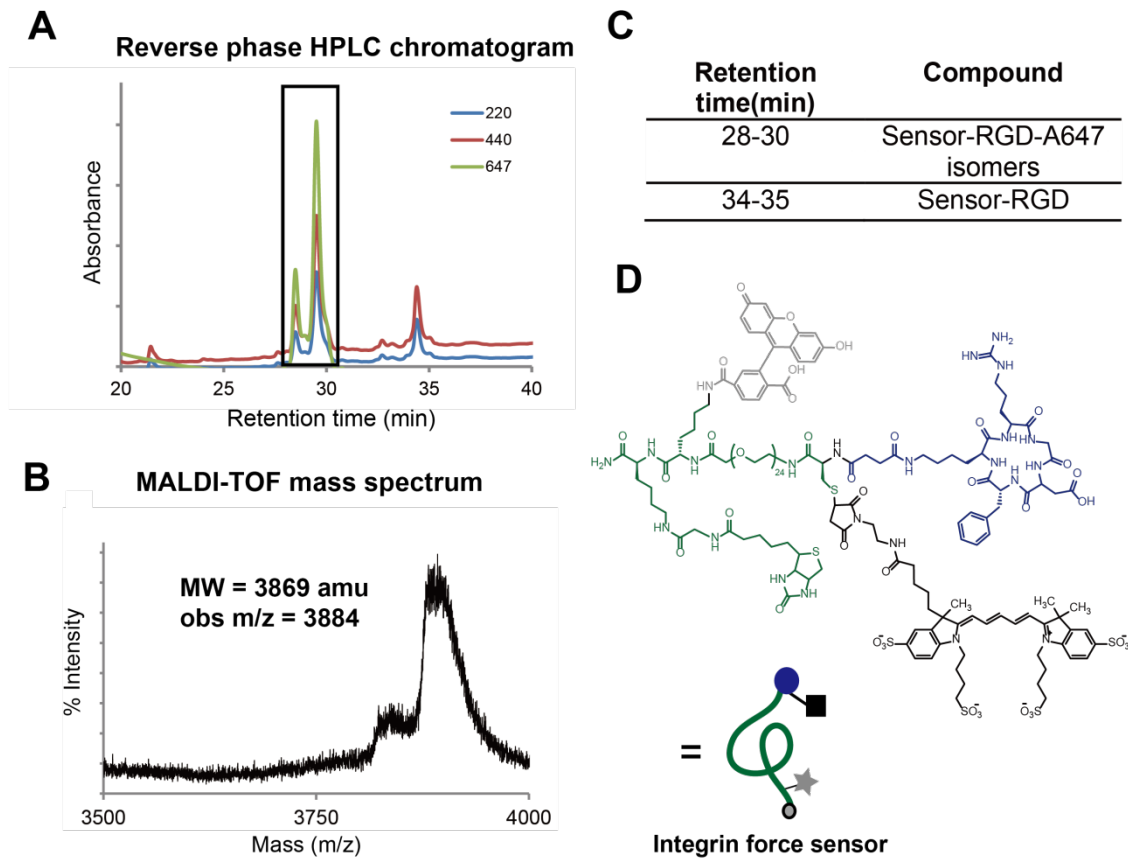
A Reverse phase HPLC chromatogram

B MALDI-TOF mass spectrum

MW = 3869 amu
obs m/z = 3884

C

Retention time(min)	Compound
28-30	Sensor-RGD-A647 isomers
34-35	Sensor-RGD

D

Integrin force sensor

Figure S6. Purification and characterization of the cRGDfK-Alexa647-PEG$_{24}$-fluorescein-biotin conjugate. (A) Reverse phase HPLC chromatogram of the cRGDfK-biotin-PEG$_{24}$-cysteine, A647 reaction mixture. The absorbance was measured at 220, 440 and 647 nm. 1 ml fractions were collected as they eluted off the column (flow rate = 1 mL/min). The peaks were characterized by MALDI-TOF MS (B) and the final integrin force sensor product (MW$_{obs}$ =3869; MW$_{expected}$=3884) was found to elute at 28-30 min (C). (D) Structure of the final product.
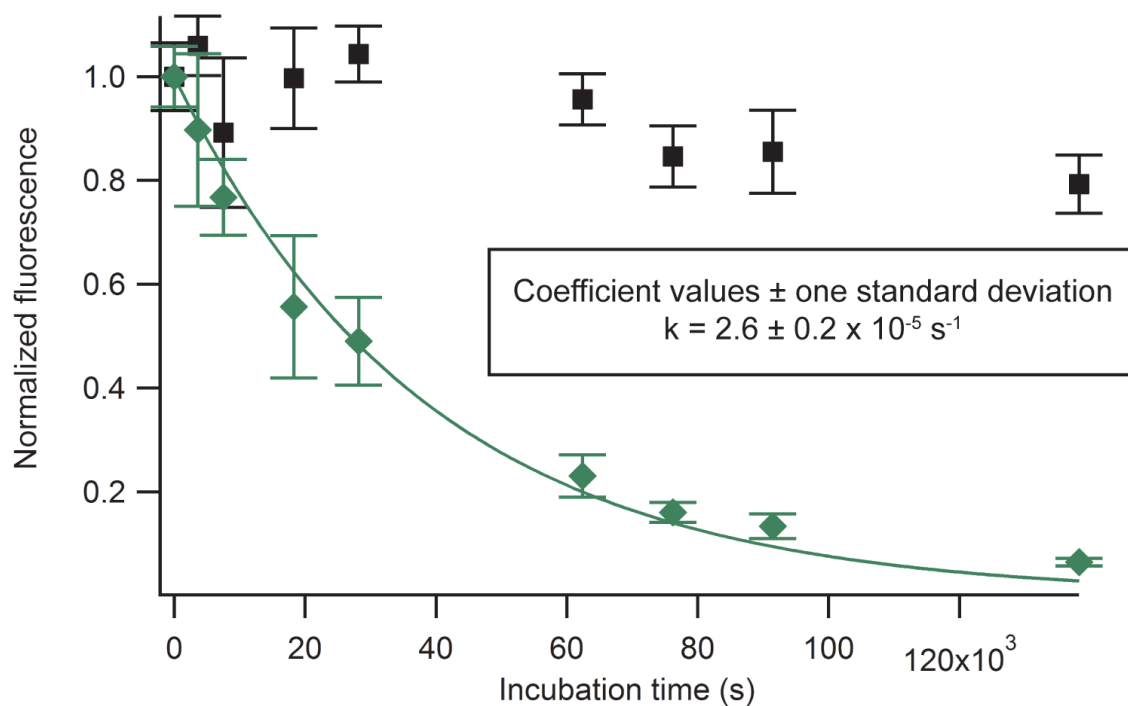
Figure S7. Determination of streptavidin-biotin dissociation rate. To determine the rate of biotin dissociation in our experiments, streptavidin modified surfaces (green diamonds) were functionalized with Alexa 488-PEG$_{23}$-biotin conjugates and then incubated with free biotin (50 nM) and imaged over a period of 33 hrs at 37 °C. Surfaces covalently functionalized with Alexa 488 (black squares) were also prepared and imaged as a control. Plot shows the fluorescence intensity of surfaces as a function of time. Error bars represent the standard deviation of fluorescence intensity from either over 40 regions across two substrates (covalent surfaces, black squares) or over 60 regions across three substrates (streptavidin-biotin surfaces, green diamonds). We used a surface preparation that was identical to the protocols described in the methods section of the manuscript. The fluorescence decay was fit to the mono-exponential function f(t) = exp(-kt) using IGOR, and yielded values of k_{off} = 2.6 +/- 0.2 x 10^{-5} s^{-1}, where the error in the k_{off} value represents the error in the fit. These values are both in agreement with rate constants reported by Deng, *et al.* (*8*) (k_{off} = 5.0 +/- 0.2 s^{-1} x 10^{-5}) and Klumb, *et al.* (*9*) (k_{off} = 4.1 +/- 0.3 x 10^{-5} s^{-1}) at 37 °C.
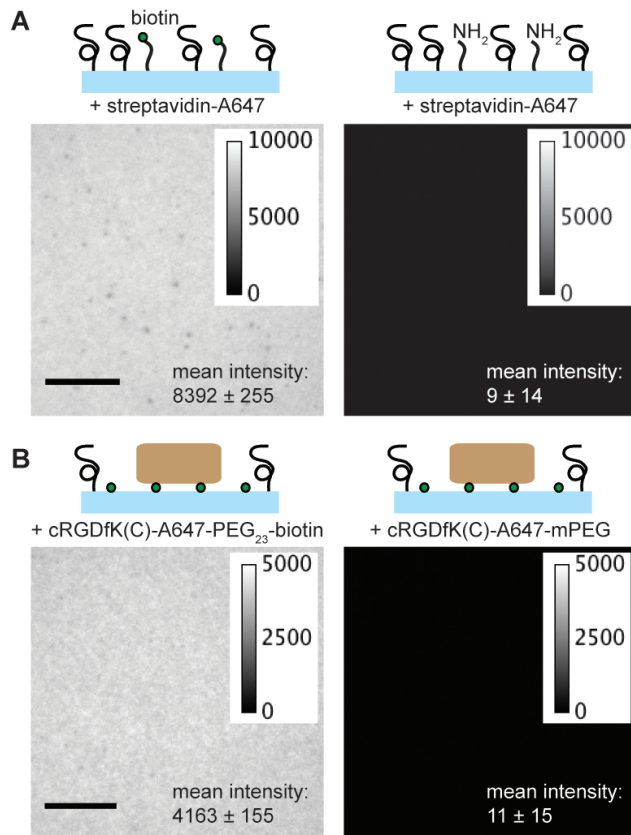
Figure S8. Force sensor conjugates are immobilized through biotin-specific interactions. A) Glass coverslips were functionalized with 1:10 amine:mPEG silanes (as described in the manuscript). The positive control surface was treated with NHS-biotin to covalently immobilize biotin, while the negative control substrate was not coupled to biotin. Both types of substrates were then incubated with streptavidin-Alexa 647 and imaged to quantify non-specific binding. This experiment showed that 99.9% of streptavidin binding occurs through specific streptavidin-biotin interaction. Mean intensities are background subtracted. B) To determine cRGDfK(C)-A647-PEG$_{23}$-biotin non-specific binding, surfaces were covalently modified with biotin and then incubated with unlabeled streptavidin (as described in the manuscript). Surfaces were incubated with cRGDfK(C)-A647-PEG$_{23}$ force reporter constructs that either included or lacked the biotin group and then were washed and imaged to determine non-specific binding of the tension reporter. This was found to be less than 0.3%. Mean intensities are background subtracted. Scale bars represent 10 μm.
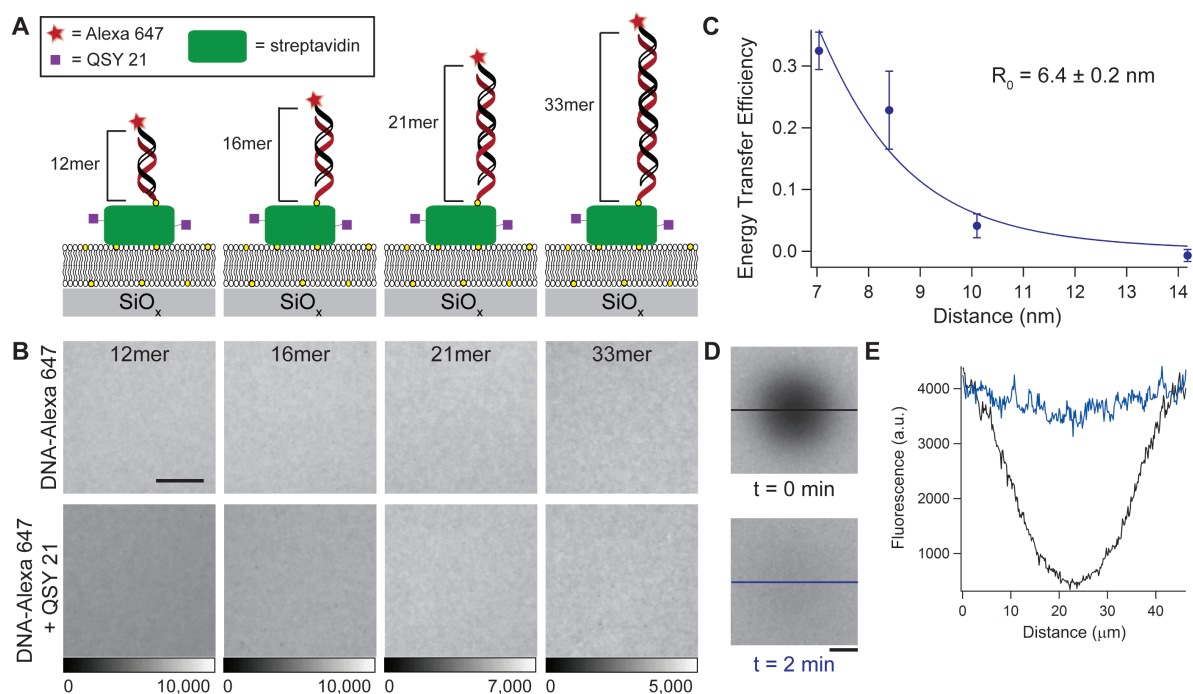
Figure S9. Calibration A to obtain the Förster distance of Alexa 647 and QSY21. Four lipid bilayer surfaces (A) were functionalized with QSY21 labeled streptavidin and then incubated with Alexa 647 labeled dsDNA of different lengths. The average fluorescence intensity for donor only surfaces (B, top row) was compared to the fluorescence intensity of surfaces containing both donor and acceptor (B, bottom row) in order to determine the quenching efficiency of the surfaces with varying fluorophore to quencher distances. The resulting efficiencies were then plotted against the known distances (C) and fit to the standard FRET equation to determine a Förster distance (R_0) of 6.4 ± 0.2 nm. All bilayer surfaces were tested for lateral mobility using FRAP experiments (D, E). Both scale bars represent 10 μm.
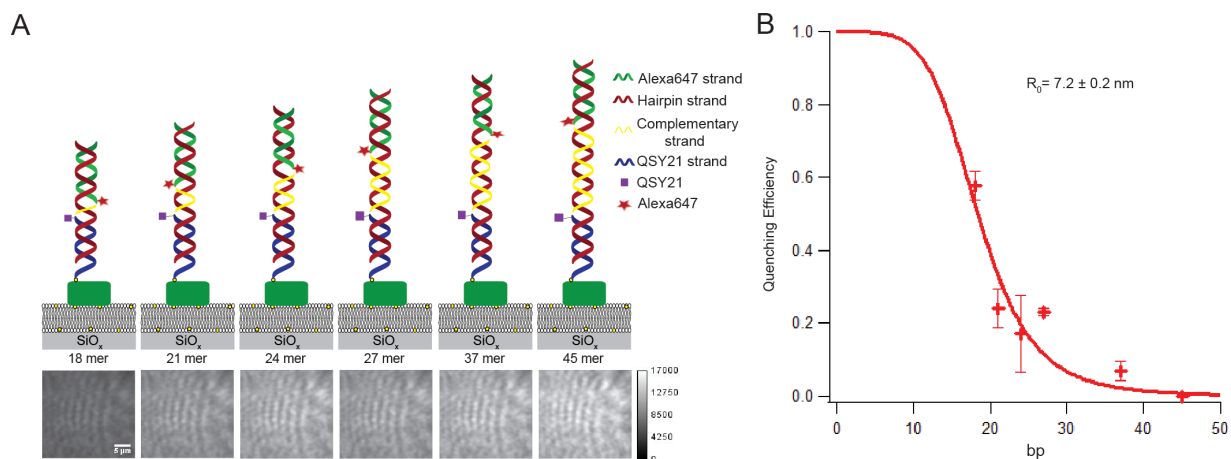
Figure S10. Calibration B to obtain the Förster distance of Alexa 647 and QSY21. (A)
Scheme of calibration experiment and representative TIRF microscopy images of the six
different hairpin oligonucleotides that were hybridized to their complementary strands. (B)
Calibration curve showing the quenching efficiency as a function of the number of base
pairs separating the fluorophore from the quencher. The data fit an R_0 value of 7.2 ± 0.2
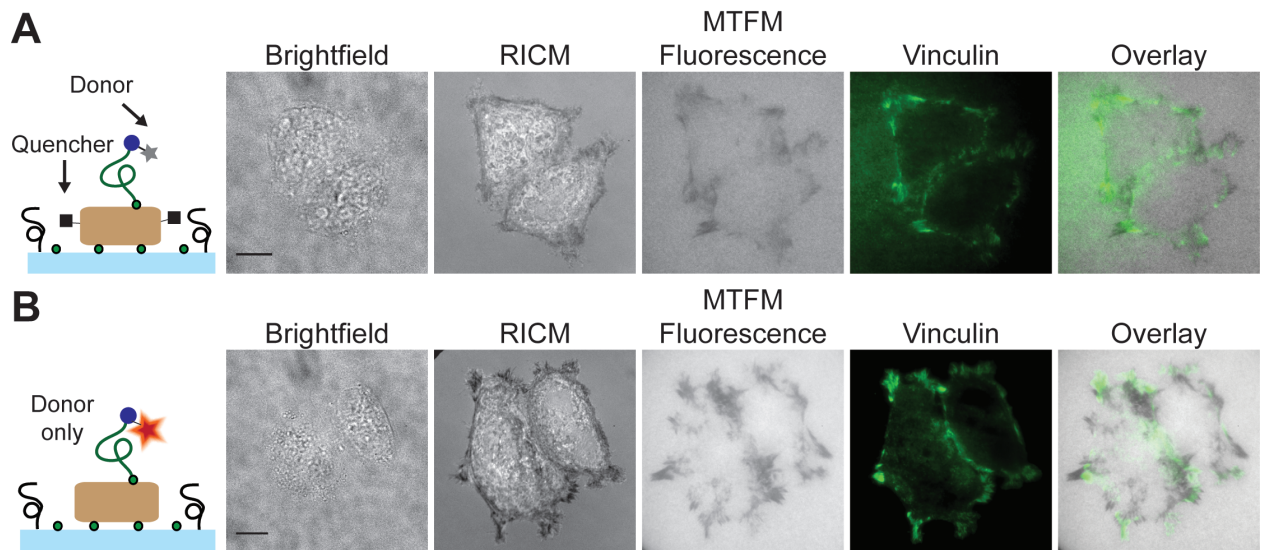nm.

A Brightfield | RICM | MTFM Fluorescence | Vinculin | Overlay

B Brightfield | RICM | MTFM Fluorescence | Vinculin | Overlay

Figure S11. Areas of decreased MTFM fluorescence colocalize with focal adhesion proteins. HCC 1143 cells were incubated for 60 min on surfaces (1:1 ratio of APTES:mPEG; 4600 streptavidin molecules/μm^2) containing streptavidin-QSY21 and cRGDfK(C)-A647-PEG$_{23}$-biotin and were subsequently fixed and immunostained for the focal adhesion protein vinculin. Scale bars represent 10 μm.
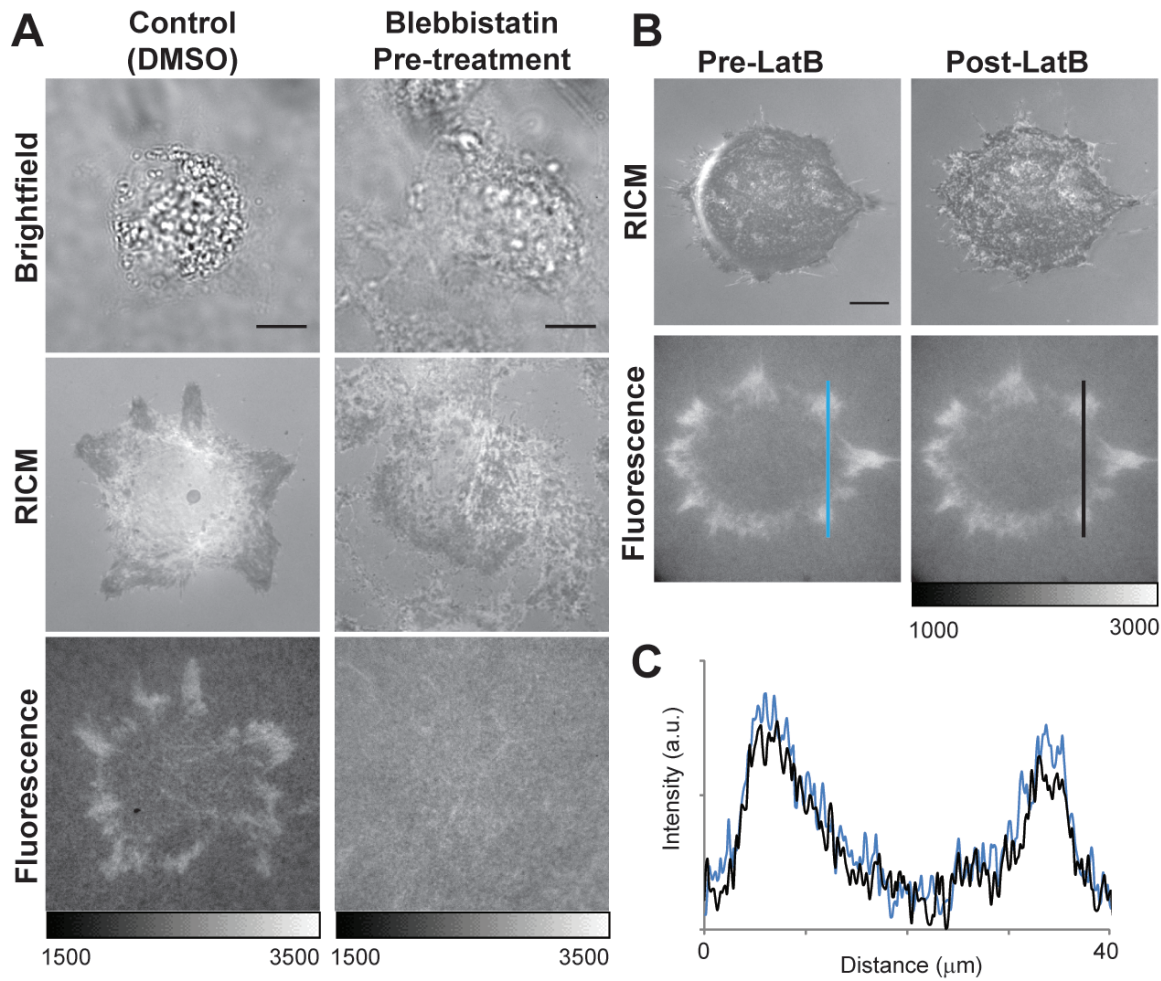
Figure S12. Biotin dissociation requires myosin and f-actin. (A) Representative brightfield, RICM, and fluorescence images of cells treated with blebbistatin (10 μM) and incubated on cRGDfK(C)-QSY21-PEG$_{23}$-biotin MTFM surface for 1 h prior to being fixed and imaged. Control cells incubated with an amount of DMSO equal to that used to add blebbistatain to the treated cells. (B) Representative images of cells allowed to incubate on cRGDfK(C)-QSY21-PEG$_{23}$-biotin MTFM surface for 30 min, imaged and then treated with 20 μM latrunculinB for 10 min. (C) Intensity profile of cell in (B) before (blue) and after (black) LatB treatment. Scale bars represent 10 μm.
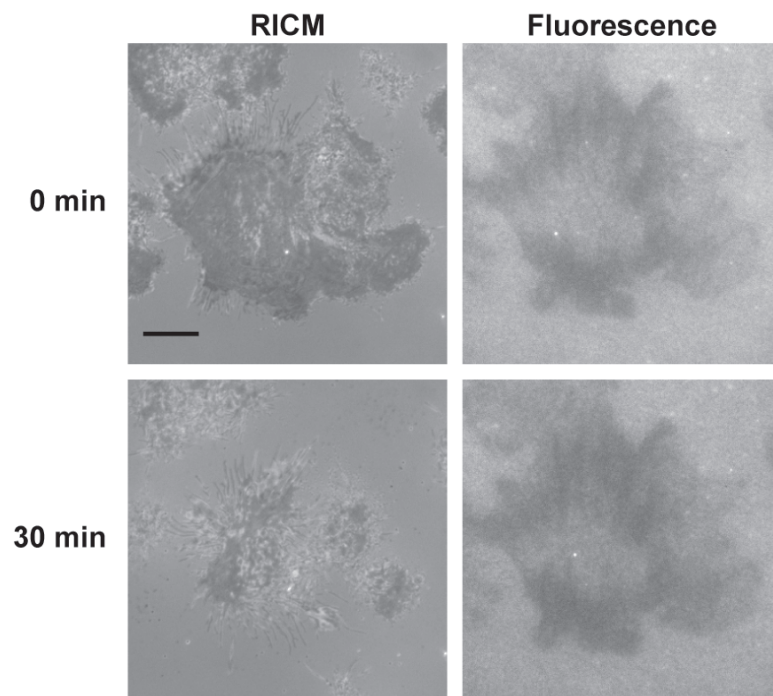
Figure S13. Cell dissociation does not reverse negative MTFM signal. Representative RICM and fluorescence images of cells incubated on a cRGDfK-Alexa647-PEG$_{24}$-fluorescein-biotin MTFM sensor surface (see Figure S8) taken prior to adding soluble cRGD peptide and 30 min after addition. RICM images indicate that cell-surface adhesion is reduced, while the negative MTFM signal remains and even decreases further during the cRGD ligand incubation. Scale bar represents 10 μm.
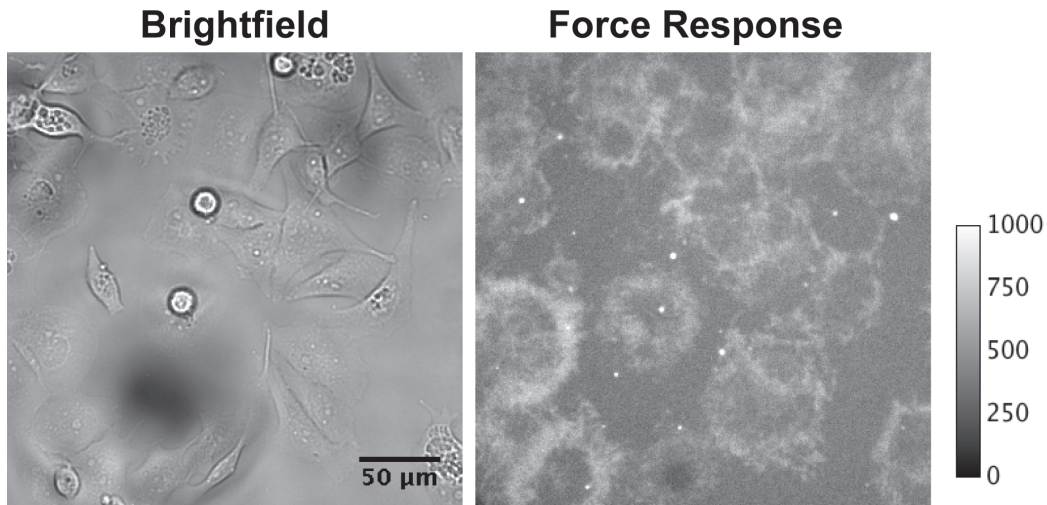
Figure S14. Global cell response to integrin MTFM sensor surface for 5 h.
HCC 1143 cells were incubated on cRGDfK(C)-QSY21-PEG$_{23}$-biotin surfaces for 5 h (1:100 ratio of APTES:mPEG; 520 streptavidin molecules/μm^2) and then imaged at 40x magnification in brightfield and epifluorescence. Fluorescence patterns at the cell edge represent regions of biotin dissociation over time.

Supporting Movies

Movie 1. HCC 1143 cells were allowed to incubate for 90 min (37 °C, 5% CO_2) on force sensor surfaces (1:10 APTES:mPEG; 4400 streptavidin molecules/μm^2) and then imaged in brightfield, RICM, and TIRFM (λ_{ex} = 640 nm) over the course of 10 min (30 sec/frame). The time lapse is rendered at 5 frames per second.

Movie 2. HCC 1143 cells were allowed to incubate for 30 min (37 °C, 5% CO_2) on force sensor surfaces (1:1 APTES:mPEG; 4600 streptavidin molecules/μm^2) and then imaged in brightfield, RICM, and TIRFM (λ_{ex} = 640 nm) over the course of 15 min (45 sec/frame). The time lapse is rendered at 5 frames per second.

Supporting References

1.   Galush, W. J., J. A. Nye, and J. T. Groves. 2008. Quantitative Fluorescence Microscopy Using Supported Lipid Bilayer Standards. *Biophys. J.* 95:2512-2519.
2.   Yun, C. S., A. Javier, T. Jennings, M. Fisher, S. Hira, S. Peterson, B. Hopkins, N. O. Reich, and G. F. Strouse. 2005. Nanometal surface energy transfer in optical rulers, breaking the FRET barrier. *J. Am. Chem. Soc.* 127:3115-3119.
3.   Clegg, R. M., A. I. H. Murchie, A. Zechel, and D. M. J. Lilley. 1993. Observing the helical geometry of double-stranded DNA in solution by fluorescence resonance energy transfer. *Proc. Natl. Acad. Sci. U.S.A.* 90:2994-2998.
4.   Norman, D. G., R. J. Grainger, D. Uhrin, and D. M. J. Lilley. 2000. Location of cyanine-3 on double-stranded DNA: Importance for fluorescence resonance energy transfer studies. *Biochemistry* 39:6317-6324.
5.   Neuert, G., C. H. Albrecht, and H. E. Gaub. 2007. Predicting the rupture probabilities of molecular bonds in series. *Biophys. J.* 93:1215-1223.
6.   Bell, G. I. 1978. Models for the specific adhesion of cells to cells. *Science* 200:618-627.
7.   Jamali, Y., T. Jamali, and R. R. K. Mofrad. 2013. An agent based model of integrin clustering: Exploring the role of ligand clustering, integrin homo-oligomerization, integrin-ligand affinity, membrane crowdedness and ligand mobility. *J. Comp. Phys.* 244:264-278.
8.   Deng, L., E. N. Kitova, and J. S. Klassen. 2013. Dissociation kinetics of the streptavidin-biotin interaction measured using direct electrospray ionization mass spectrometry analysis. *J. Am. Mass Spectrom.* 24:49-56.
9.   Klumb, L. A. C., V.; Stayton, P.S. 1998. Energetic roles of hydrogen bonds at the ureido oxygen binding pocket in the streptavidin-biotin complex. *Biochemistry* 37:7657-7663.
10.   Goldmann, W. H. 2000. Kinetic determination of focal adhesion protein formation. *Biochem. Biophys. Res. Comm.* 271:553-557.
11.   Plotnikov, S. V., A. M. Pasapera, B. Sabass, and C. M. Waterman. 2012. Force fluctuations within focal adhesions mediate ECM-rigidity sensing to guide directed cell migration. *Cell* 151:1513-1527.